Constraints on the nature of the blazar S5 0716+714 optical radiating region obtained from the long-term variability

M.A. Gorbachev[1,2], M.S. Butuzova[2], A.V. Zhovtan[2], S.G. Sergeev[2], S.V. Nazarov[2]

[1]*Kazan (Volga Region) Federal University,* [2]*Crimean Astrophysical Observatory of RAS*

Introduction

Multiband optical photometry data of blazar S5 0716+714 obtained from 2002 to 2019 at CrAO reveal stable color index change with variability. We analyzed this trend under variability caused by the Doppler factor change in the presence of a curved photon energy spectrum. We considered that curved photon spectrum is due to either a break in the energy spectrum of emitting electrons, which is caused by radiative losses, or the synchrotron self-absorption acting in a compact jet part of the jet.

Optical data

Optical observations were performed in B-, V- R-, I-band by 70-cm telescope AZT-8 of Crimean astrophysical observatory (Fig. 1).

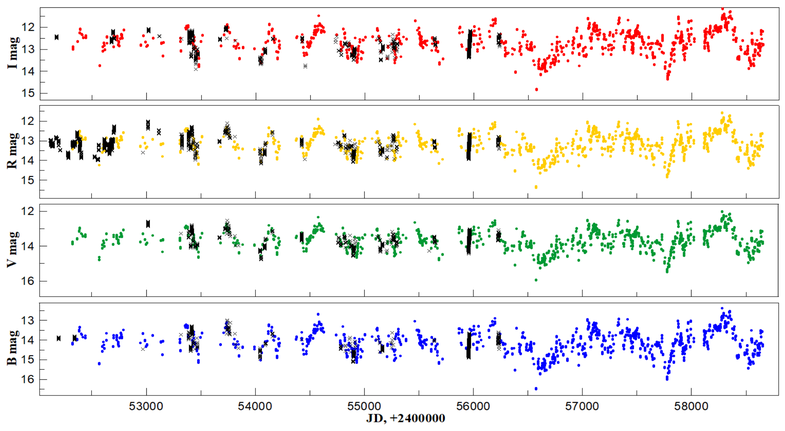

Fig. 1. Optical light curves for S5 0716+714. Color markers denote AZT-8 data in the different bands, black markers show other published data.

Flux-flux dependencies are well approximated by straight lines (Fig. 2). This fact indicates the existence of one predominant process responsible for long-term variability.

Using linear fitting data, we calculated the change in the spectral index α with variability (Fig. 3). It can be seen that the bluer-when-brighter trend appears. And the highest changes in α occur at low fluxes, and in the bright condition of the object, the color index practically does not change.

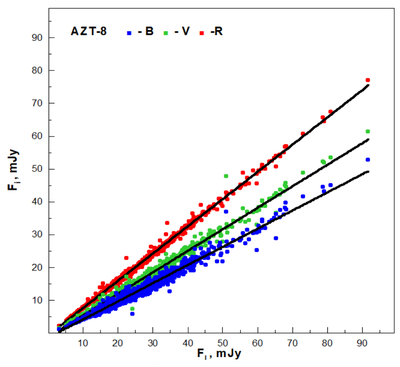

Fig. 2. Flux-flux diagram plotted based on AZT-8 data.

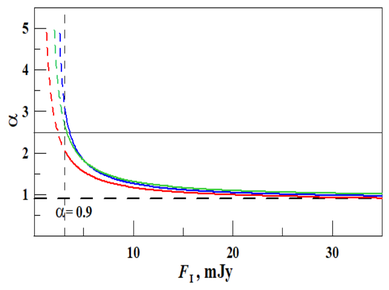

Fig. 3. The change of the object spectral index under variability.

To analyze how fully the geometric effects in the curved radiation spectrum explain the observed properties of the variability, we simulate the variability under different assumptions about the emitting regions and compare the obtained points with the observed dependence α (F_I) calculated from the lines that fit the data (Fig. 4). In this case, we use the values of the flux of the slowly changing (constant) component of variability F_I = 10, 15, and 20 mJy, which match the Doppler factor 5, 6, and 7. The spectral index of this component is assumed to be α_c = 1.5.

Note that the values with $F_I \le 10$ mJy are about 6% of the total number of points and fixed for a short time interval. At $F_I \le 10$ mJy, the spectrum of an object is steep and can be associated with a constant component, when the object is in a dim state, the emitting electrons are strongly cooled, and the contribution from the variable component is extremely small.

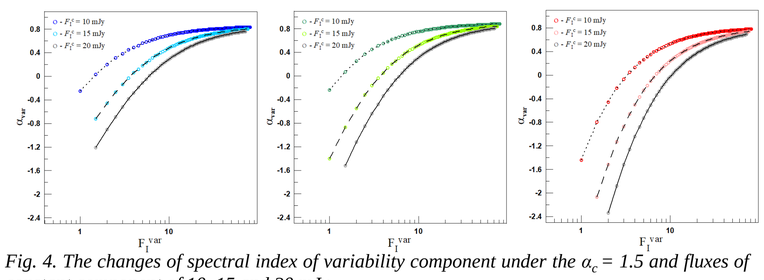

Fig. 4. The changes of spectral index of variability component under the α_c = 1.5 and fluxes of constant component of 10, 15 and 20 mJy.

Case of synchrotron self-absorption

The action of synchrotron self-absorption in the radio range has been confirmed for several hundred sources [1]. Extrapolating this result to optical frequencies, we assume that the all observed flux comes from the jet region, in which the medium becomes transparent to optical radiation (the optical core). The schematic spectrum of the optical core in the source reference frame is shown in Fig. 5.

One emission region

Assuming that there is a single radiating region, we assume that the radiation of the constant component comes from an optically thin medium characterized by a Doppler factor δ_c. In the jet stream, development is possible (magneto)hydrodynamic instabilities and turbulence, because at some time a part of the radiating region may increase δ due to a decrease in the angle between the velocity vector of this part with the beam of view and/or an increase in velocity, which will lead to an increase in the flux in the observer's reference frame and a change in the overall spectral index. We take the parts of the radiating region with the increased δ as the variable component.

In the simulation, we changed δ_{var} in the range from δ_c to 50, a parameter that characterizes the ratio of the normalizing constants in the expression for the flux of a constant and variable component, D from 0.1 to 1, the frequency for which the optical thickness of the medium is equal to one, ν'_1 from 10^{13} to 10^{14} Hz.

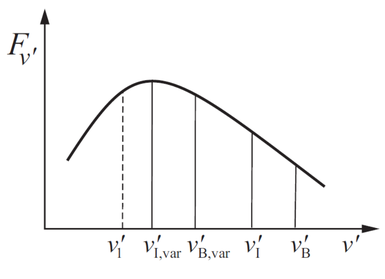

Fig. 5. Scheme of the spectrum of the emitting region in synchrotron self-absorption. Marked are the frequencies of the constant and variable components, the radiation at which falls within the observed range.

When the Doppler factor changes, the component of the magnetic field perpendicular to the line of sight changes **[2]**, which leads to a change in ν'_1 in some small interval **[3]**. To select the values of ν'_1 to be used in further analysis, we compare the observed F_I^{obs} distribution with the theoretical F_I^{th}. Under this, we combine the theoretical points obtained for the considered pairs B-I, V-I, R-I at the fixed ν'_1. The simulated points corresponding to the frequencies ν'_1 at which the best match is observed (Fig. 6) were selected for further analysis.

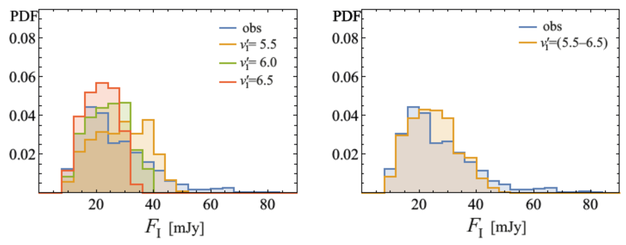

Fig. 6. The observed and theoretical distributions of F_I for the fixed ν'_1 (left) and the interval of ν'_1 (right).

We have obtained the characteristics of the variable component, which are necessary to explain the observed properties of the variability (Fig. 7):
- δ_{var} varies from 7 to 13; the discrepancy between the lower bound and the value of δ_c implies the existence of selected directions in the jet flow, which is unlikely.
- The maximum spectral index is ≈0.8, which does not correspond to the initial assumption.

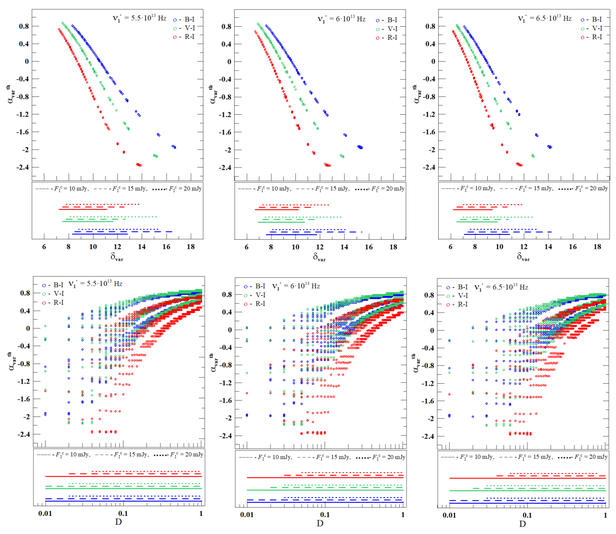

Fig. 7. The obtained properties of the variable component. The points obtained from the filter pairs B-I, V-I, and R-I are marked in blue, green, and red, respectively. The lines at the bottom panel of each plot indicate the range of the corresponding parameter.

Two emission regions

Suppose there are two radiating regions. One is the region with synchrotron self-absorption acting. Because of its compact size, this region will be considered as a variable component. The second region is an extended jet with an optically thin medium. Jet radiation is associated with a constant component.

There are two possible cases, illustrated in Fig. 8:
1) the spectra of the constant component α_c and the optically thin part of the variable α_{pl} components are equal;
2) the spectrum of the constant component corresponds to the emission spectrum of electrons that have experienced high energy losses through radiation ($\alpha_{pl} = \alpha_c - 0.5$) as the electrons propagate into the jet.

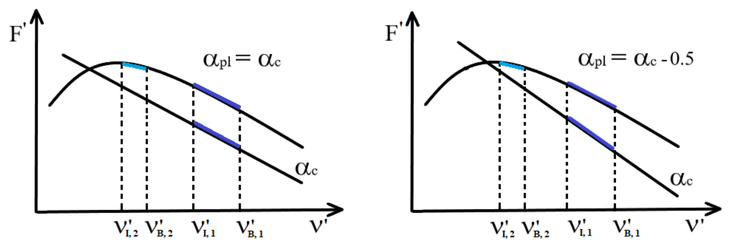

Fig. 8. Schemes of the spectra of the constant and variability components. The blue color indicates the frequency range of the variable component, the radiation at which falls within the observed range due to $\delta_{var}>\delta_c$ under the absence of radiation energy losses by electrons (left) and for high radiation losses (right).

Note that the same intensity of the constant component in the source reference frame will create both a dim jet with a large Doppler factor δ_c=15, and a bright jet with a small Doppler factor δ_c=5. We are considering both of these possibilities.

Two emission regions, case 1

The results of selection ν'_1 and modeling the properties of the variable component are shown in Fig. 9 and 10, respectively.

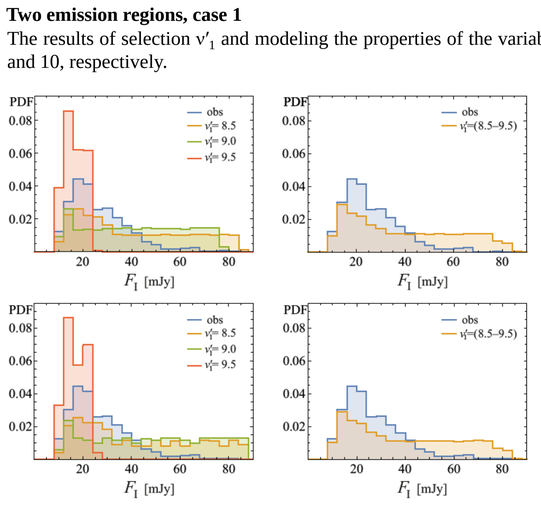

Fig. 9. Probability density distributions for observed and theoretical fluxes for the bright (top panel) and dim (bottom panel) jet. The distributions for fixed frequencies and frequency intervals are displayed at the left and right panels, respectively.

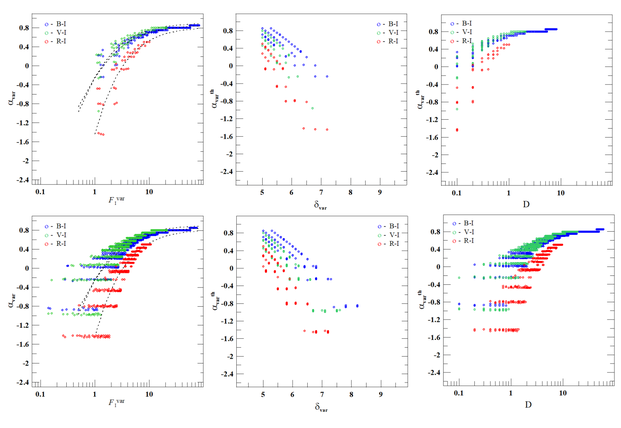

Fig. 10. Illustration for parameters of variable components for bright (top panel) and dim (bottom panel) jet.

The simulation does not allow us to give an advantage to any of the considered assumptions about the jet Doppler factor.

Two emission regions, case 2

Let us turn to the case in which the electrons, as they moved from the region of the optical core to the jet, underwent strong radiative changes. The results of selecting ν'_1 and modeling the properties of the variable component are shown in Fig. 11 and 12, respectively.

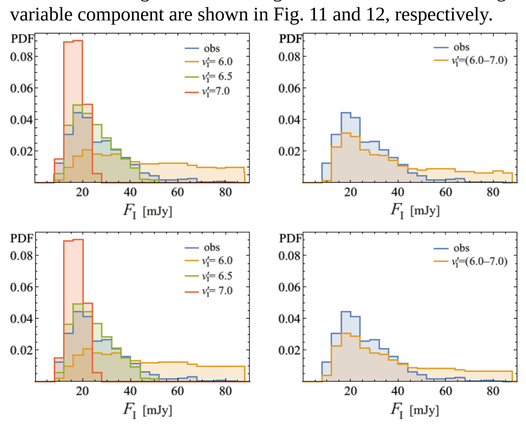

Fig. 11. Probability density distributions for observed and theoretical fluxes for the bright (top panel) and dim (bottom panel) jet. The distributions for fixed frequencies and frequency interval are displayed at the left and right panels, respectively.

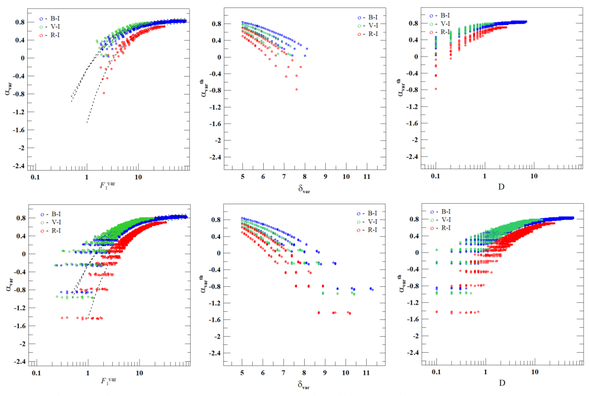

Fig. 12. Illustration for parameters of variable components for bright (top panel) and dim (bottom panel) jet.

The simulation results do not show significant differences from the previous case. The answer to the question of the preference of one case over another can be obtained from the estimation of the magnetic field.

Magnetic field

Assuming that synchrotron self-absorption occurs in a region with a size of one gravitational radius of a black hole with mass M_{BH}= 10^8 and $5\cdot10^8$ $M_\odot$, we estimated the magnetic field $B_\perp$ for the three cases considered (Fig. 13, 14). In the case of two emission regions (case 2), $B_\perp$ takes acceptable values for both bright and dim jet.

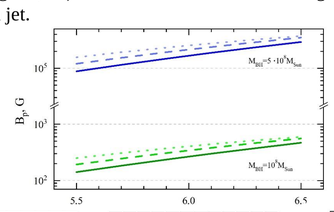

Fig. 13. $B_\perp(\nu'_1)$ for the case of a single emitting region. The solid, dashed, and dotted lines show the dependencies for F_I^c= 10, 15 and 20 mJy, respectively.

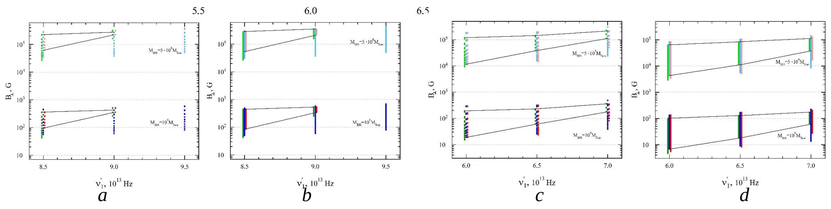

Fig. 14. $B_\perp(\nu'_1)$ for the bright (a, c) and dim (b, d) jet under $\alpha_{pl}=\alpha_c$ (a, b) and $\alpha_{pl}=\alpha_c$–0.5 (c, d). Blue, green, and red colors denote the values of $B_\perp$, obtained for the filter pairs B-I, V-I, and R-I, respectively. The lines connect the boundaries of the intervals of $B_\perp$ values at a fixed ν'_1.

Case of broken power-law electron spectrum

The energy loss of the electron energy through radiation leads to a break in the power-law particle spectrum. If, at a minimum δ_{var}, the frequencies marked in Fig. 15 by red color fall within the observed range, then as the δ_{var} increases, the frequency interval shifts to the left. The α_{var} values vary from α_c in the dim state to α_c – 0.5 at the maximum brightness of the object.

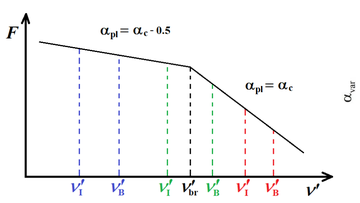

Fig. 15. The emission spectrum with a break in the source reference frame.

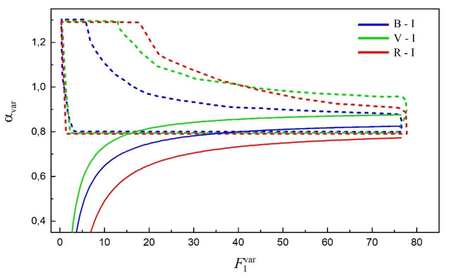

Fig. 16. The results of α_{var} simulating for a break in the radiation spectrum. Dashed lines mark the areas containing the model points. The solid lines of the corresponding colors show the dependence of the α_{var} obtained from the observations

Fig. 16 shows that the correspondence between the observational data and the simulation is achieved only at large values of the flux of the variable component.

Conclusion

The flux-flux diagrams based on the B-, V-, R-, and I-photometry data for blazar S5 0716+714 show a well-defined dependence during more than 20 years. From the considered assumptions on the emitting region, it is most likely that the radiation comes from two jet regions. One of them is a core, which is a compact region in which synchrotron self-absorption acts and locates near the true jet base, and the other one is a more distant extended jet with an optically thin medium. Under this, the electrons experience significant radiative losses before they propagate into the jet. The contributions from the core and jet in the observer's reference frame are comparable.

Acknowledgments

The all theoretical part of this investigation was supported by the Russian Science Foundation grant No. 19-72-00105.

Contact email

mgorbachev17@gmail.com

References

1. B. Pushkarev, T. Hovatta, Y. Y. Kovalev, M. L. Lister, A. P. Lobanov, T. Savolainen, J. A. Zensus, MOJAVE: Monitoring of Jets in Active galactic nuclei with VLBA Experiments. IX. Nuclear opacity, A&A545 (2012) A113.
2. M. Lyutikov, V. I. Pariev, D. C. Gabuzda, Polarization and structure of relativistic parsec-scale AGN jets, MNRAS360 (3) (2005) 869–891.
3. A. G. Pacholczyk, Radio astrophysics. Nonthermal processes in galactic and extragalactic sources, San Francisco: Freeman, 1970.